Available online at www.sciencedirect.com

ScienceDirect

Procedia CIRP 71 (2018) 232–237

www.elsevier.com/locate/procedia

4th CIRP Conference on Surface Integrity (CSI 2018)

Influence of cutting edge asymmetry on grain refinement of Ti6Al4V

Eric Segebade[a,*], Daniel Kümmel[b], Frederik Zanger[a], Johannes Schneider[b], Volker Schulze[a]

[a]wbk Institute of Production Science, Karlsruhe Institute of Technology (KIT)
[b]IAM Institute for Applied Materials, Karlsruhe Institute of Technology (KIT) and MicroTribology Center μTC

* Corresponding author. Tel.: +49-721-608-45906 ; fax: +49-721-608-45004. *E-mail address:* eric.segebade@kit.edu

Abstract

Asymmetrical cutting edges have been proven to influence the resulting surface layer states of machined metal parts. As machining of Ti6Al4V alloy is subject to rather high tool wear, tool geometry changes during machining can influence the resulting surface layer states like residual stresses and nanocrystalline surface layer depth. In this paper, the influence of asymmetric cutting edge microgeometries (characterized by form-factor) and different process parameters on the resulting surface layer microstructure of Ti6Al4V is investigated through face turning experiments and focused ion beam analyses. 2D-FE simulations are conducted using the software Simufact Forming, and a Johnson-Cook model with triaxiality based damage criterion. According to the known mechanisms of grain refinement, mechanical and thermal states are analyzed and related to the experimental data. Relative roundness higher than one, and form-factors smaller than one lead to severe surface layer deformation and increased recrystallization depths, with the effect of form-factor clearly dominating compared to relative roundness.

Selection and peer-review under responsibility of the scientific committee of the 4th CIRP Conference on Surface Integrity (CSI 2018).

Keywords: Cutting Edge; Surface Integrity; Tool Microgeometry

1. Introduction

Surface integrity (SI) influences a range of key part performance indicators including but not limited to wear resistance, fatigue strength, and corrosion resistance. While the prediction of resulting topography is usually done analytically, internal features such as residual stresses, and microstructure require more in depth techniques like Finite Element Method (FEM) models. Over the years, different SI features were addressed using different software packages and underlying material and friction models. For instance, Özel et al. predicted residual stresses [1], Umbrello et al. modelled machining induced hardness and grain size changes [2], and Buchkremer et al. investigated grain refinement of the surface layer when machining AISI 4140 with a model considering mechanical and thermal energies [3]. It was also proven, that the asymmetry of the cutting edge greatly influences the resulting surface integrity [4, 5]. It thus, among other features, changes the resulting thickness of the nanocrystalline (NC) and microcrystalline (MC) layer [6]. This is of special interest for materials like Ti6Al4V associated with tool wear, because surface conditioning by machining gets harder to control as the boundary conditions of the surface generating part of the cutting tool change.

A number of methods to characterize cutting edge microgeometries exist in literature. For instance, Wyen et al. analyze and compare different ways of characterization while suggesting their own method, driven by the aim to reduce measurement uncertainty [7]. Another possibility is the form-factor method by Denkena et al. [4]. In its basic form, it constitutes an easy comparison of simplified tool microgeometries. Apart from the asymmetry, relative roundness is also important for the generation of surface integrity features like NC and MC layers. It is defined as the ratio of the cutting edge radius r_β and the cutting depth h (orthogonal cutting). A large relative roundness is known to influence the workpiece up to a larger depth due to ploughing effects [8].

In this work, the machining induced grain refinement of Ti6Al4V is investigated with regard to cutting edge asymmetry and relative roundness. While face turning experiments offer a quantitative insight into the trends of the

Selection and peer-review under responsibility of the scientific committee of the 4th CIRP Conference on Surface Integrity (CSI 2018).
10.1016/j.procir.2018.05.065

NC and MC-layers after machining, 2D FEM simulations add a qualitative assessment of the change within the thermo-mechanical load collective induced by the asymmetry and relative roundness when machining Ti6Al4V.

2. Experiments and analyses

Experiments were conducted using Ti6Al4V Ø 25 mm round bars in aerospace application standard condition. Uncoated DNMG 150612 inserts from Walter Tools with a nominal edge radius r_β = 40 µm were used for face turning on an Index V100 vertical turning center. The machine features a fixed tool with the rotating spindle moving on three axes. After a pre-cut of 0.3 mm depth in lubricated condition, the respective experimental cutting depth was applied. Cutting depths and form-factors are shown in Fig 1. The parameters enable an analysis of the effect of cutting depth a_p (nearly constant form-factor) and asymmetry (constant cutting depth). Cutting forces were recorded during the experiments (Kistler). Roughness was measured in radial direction using a perthometer (Mahr).

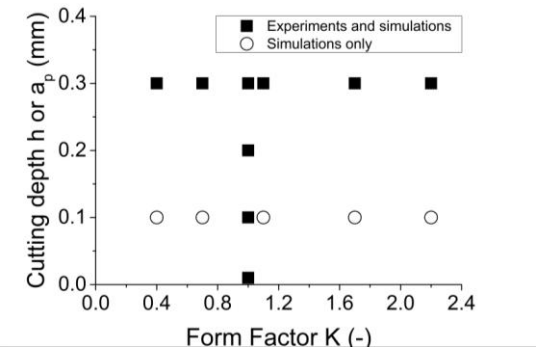

Fig 1. Face turning experiments and 2D simulations: v_c = 160 m/min; f = 0.1 mm/rev.

Cutting edges were measured along the tool nose radius by confocal microscopy (Nanofocus) before the process. Characterization was done using the form-factor. Controlled radii and asymmetries were achieved by stream finishing (OTEC). The microgeometries are listed in Table 1. Form-factors of 1 thus correspond to a certain relative roundness r_β/h in the simulations with varying h. Additionally, the interaction of asymmetry and cutting depth was only analyzed in simulations.

Specimens were prepared from the outer regions of the produced discs. The specimen´s resulting NC and MC surface layers were subsequently analyzed parallel to the cutting direction by Focused Ion Beam (FIB). Layers were discerned by the largest observed grain size (g_s) considering both viewable directions along five randomly chosen vertical lines. The following criteria where applied:

- Nanocrystalline: $g_s < 0.1$ µm
- Microcrystalline: $g_s < 1.0$ µm

The microcrystalline layer depth thus includes the nanocrystalline layer depth. Usually, saw tooth-chipping leads to an uneven layer depth along the surface. Below the MC layer, shearing can still be observed. The layer of sheared grains larger than 1.0 µm was not considered in this work.

Table 1. form-factor K and correlating segment lengths S_γ and S_α along the nose radius of the tools used in this work (Type DNMG 150612).

No.	K [-]	S_γ [µm]	S_α [µm]
0 (reference)	1.0	40 ± 1	40 ± 1
1	2.16	68	31
2	1.70	55	32
3	1.12	42	37
4	0.73	40	54
5	0.36	38	107

3. Modelling and simulations

A 2D model of orthogonal cutting was set up and calculated as per Fig 1 using the software Simufact Forming. A Johnson-Cook material model was implemented via a subroutine. Parameters from [9] were used. Additionally, the triaxiality based Johnson-Cook failure model from [10] was programmed using parameters from [11]. The workpiece was modelled with 5 mm length and a deformable area of 300 µm below the cutting edge. A local mesh refinement to 1.5 µm element edge length was enforced beneath the cutting edge radius from the surface down to 30 µm depth. Below this area, the edge length was increased to first 3 µm down to 50 µm, 6 µm down to 150 µm and 12 µm for the rest of the workpiece. Remeshing was enforced every 5 increments.

A rake angle of 3.5° was assumed, considering the tool geometry with a nominal wedge angle of 83° near the cutting edge, and the nominal clearance angle of the tool holder of 3.5°. All tools were modelled with their respective microgeometry reduced to elliptical asymmetry as per Table 1 and used with respective cutting depths as per Fig 1. A combined friction model was applied for all simulations (µ = 0.35; m = 0.7). The resulting relative roundness for form-factors of 1 is listed in Table 2. For asymmetrical edges, using this parameter is not possible, since the mean radius does not offer great insight into the geometry, and choosing an edge segment length would not lead to a relevant classification. Furthermore, the calculation of relative roundness is valid for orthogonal conditions only, and thus is connected to the simulations rather than the experiments in this work, which are defined by the cutting depth a_p.

Table 2. Resulting relative roundness for the simulations at K = 1 with r_β = 40 µm and different cutting depths h.

Cutting depth h [mm]	Relative roundness r_β/h [-]
0.3	0.13
0.2	0.2
0.1	0.4
0.01	4.0

The time dependency of the saw tooth formation hinders analyses of strain rates and temperatures, because a full analysis per increment would be necessary to receive a full overview of the process. An analysis of deformed volumes during steady state as done in [6] was thus not possible in this

work. This is why the time of influence (t_i) of strain rates above 10^5 1/s was analyzed instead. Additionally, the maximum temperature at all integration points across all increments was captured by the subroutine. Thus, not just the depth of strain, but also the evolution of strain through influencing time t_i, and local peak temperatures could be analyzed at the end of the 1 mm length of cut. Figure 2 shows an example of local peak temperatures inside the workpiece for K = 1 and h = 0.3 mm after 1 mm length of cut. Fig 3 shows the relatively small influence of shear banding on the resulting influencing time within the surface layer. Values were taken along a 50 µm track along the surface in order to use a mean value.

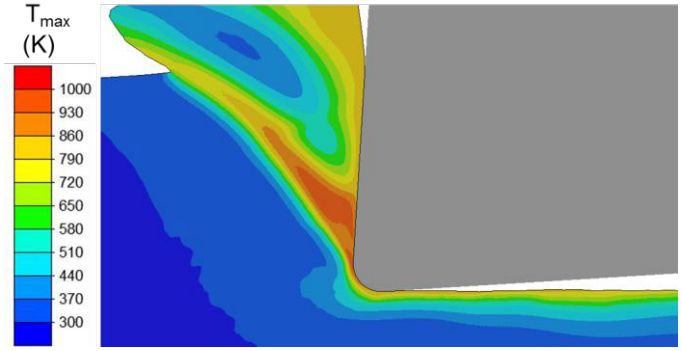

Figure 2: Local peak temperatures in K, K = 1; v_c = 160 m/min, h = 0.3 mm, after 1 mm length of cut.

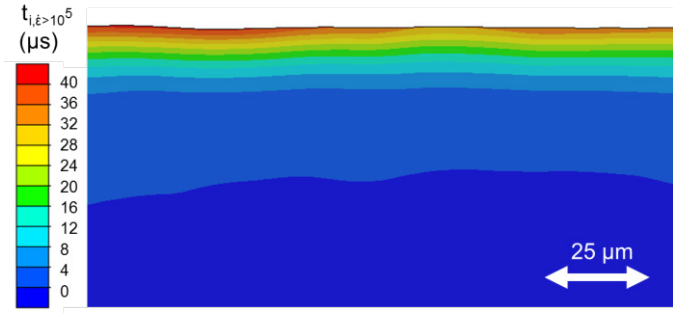

Fig 3. Local influencing time in µs, K = 1; v_c = 160 m/min, h = 0.3 mm, after 1 mm length of cut, 250 µm behind the cutting edge.

4. Results and discussion

The measured forces are shown in Fig 4. Forces generally drop with decreasing depth of cut with a constant form-factor (black). At a constant cutting depth and variable form-factor (red), the minimum of all force components was observed using a form-factor of 1.7, while the maximum was found for the smallest form-factor of 0.36. In particular, the passive force more than doubled compared to the results of experiments with larger form-factors. Fig 5 analogously shows the relative forces calculated from the process forces. The relative forces only change significantly at a cutting depth smaller than the cutting edge radius (black, a_p = 0.01 mm, r_β = 40 µm). At these parameters, the passive force is high compared to the cutting force, while the range of the feed force during the process increases (see error bars). Cutting conditions of this kind can be considered extreme regarding the chip formation. The effect of edge asymmetry at constant cutting depth (red) is most severe for K < 0.4, increasing the ratio of passive and feed force to cutting force. In spite of the extreme cutting conditions, roughness of all samples was within Ra 0.3-0.4 µm and Rz 1.4-2.7 µm, with higher Rz to be found for form-factors larger than 1.

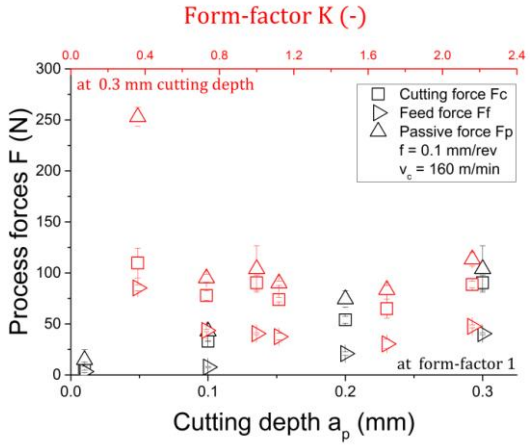

Fig 4. Forces measured in face turning experiments.

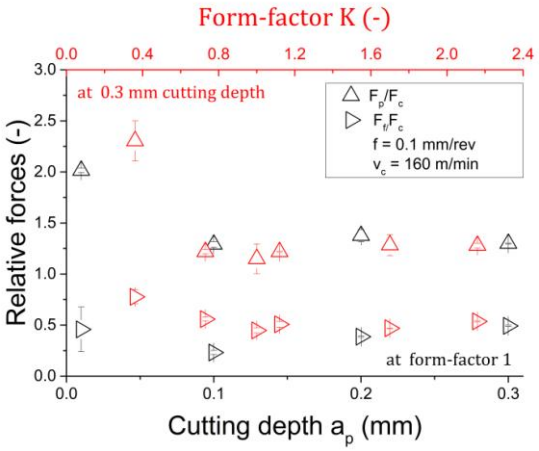

Fig 5. Relative forces measured in face turning experiments.

When comparing the measured relative forces with the resulting nano- and microcrystalline layer depth, as shown in Fig 6, a general correlation can be deduced: Higher feed and passive force in relation to cutting force lead to a deeper surface layer affected by grain refinement. The comparison also suggests, that the effect of edge asymmetry on grain refinement is more severe than the effect of small cutting depth (red, low form-factor vs black, low cutting depth). At the same time, the variance of NC layer depth achieved by form-factor is considerably larger than that achieved by relative roundness (see error bars). The FIB analysis of the two extremes of K investigated in this work are shown in Fig 7.

On the one hand, experience from symmetric cutting edges suggests, that this is due to enhanced ploughing effects, which in the case of saw tooth chipping seem to be less stable than in steels. On the other hand, previous simulation based analysis (AISI4140) showed a simultaneous reduction of peak strain rates and an increase of influenced volume at moderate strains (10^3 1/s) for low form-factors [6].

The intensity and depth of strain was regarded as depicted in Fig 8 for a strain > 10 along (mean value of 5 positions). All results fall into the range of 3 to 6 µm, with a trend towards a deeper affected layer at higher form-factors, especially with low cutting depth. The lowest cutting depth of 0.01 mm features the deepest depth of strain > 10 (largest relative roundness of $r_\beta/h = 4.0$).

Looking at Fig 9, a similar trend can be observed for the influencing time of strain rates above 10^5 1/s. Again, no clear correlation between strain rates and resulting NC or MC layers of the experiments is apparent apart from the effect of relative roundness (if considered in conjunction with cutting depth a_p). In spite of the form-factor of 0.36 clearly leading to a deeper refined surface layer in the experiments, neither strain nor strain rate seem to be responsible in this case. Still, the passive and feed force increase considerably in relation to the cutting force in both instances.

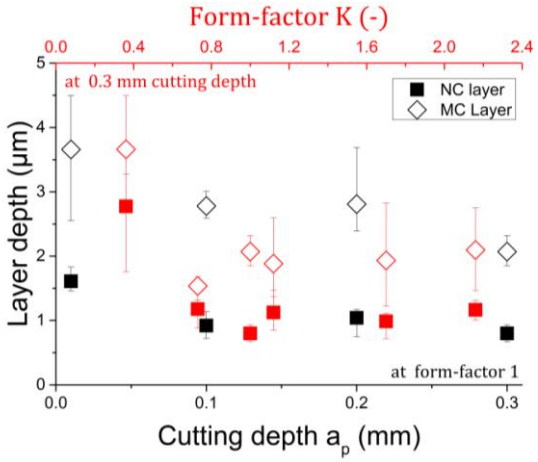

Fig 6. Measured grain refinement; v_c = 160 m/min; f = 0.1 mm/rev.

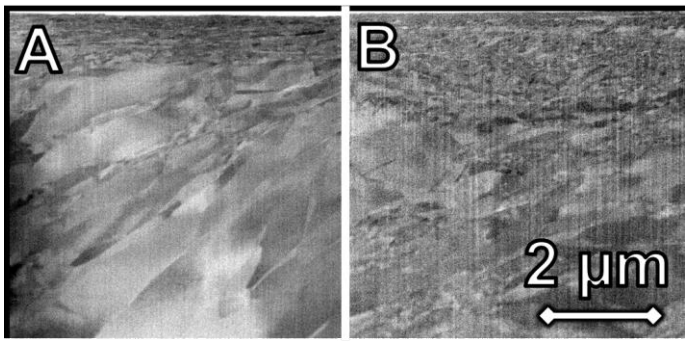

Fig 7 . Focused-Ion-Beam analysis: A: K = 2.16; B: K = 0.36

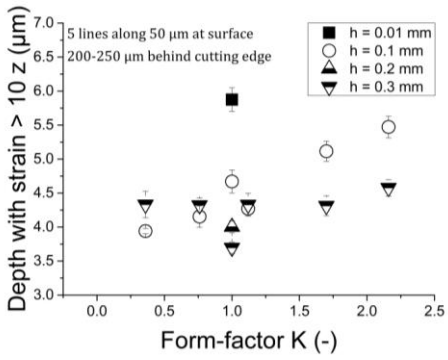

Fig 8. Depth of strain greater than 10 in all simulations.

When plotting the maximum temperature along the depth beneath the surface as in Fig 10 for K = 1, in Fig 11 for variable K at h = 0.3 and in Fig 12 for variable K at h = 0.1, the form-factor of 0.36 at 0.3 mm depth of cut clearly shows an offset. The peak temperature at the surface is roughly 50 K higher than for the other form-factors at this cutting depth. It actually reaches its highest value (more than 150 K above the other simulations) some 5 µm below the surface.

In contrast to this, the temperature at the largest relative roundness at 0.01 mm cutting depth (Fig 10) is close to 100 K below all other surface values taken from the simulations. It is interesting to note, that no significant difference in surface temperature was observed for the simulations with K = 1 at cutting depths of 0.1 mm and above. This is in spite of clearly differing maximum temperatures in the shear bands. Highest temperatures in the shear bands were observed at 0.3 mm cutting depth for the simulations conducted in this work.

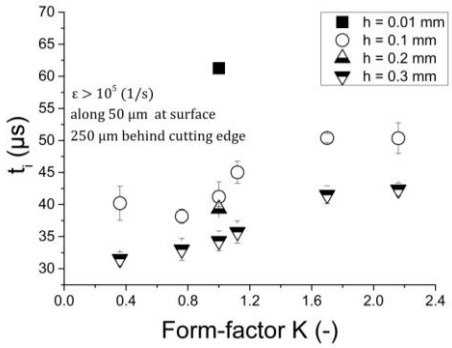

Fig 9. Influencing time t_i of strain rate $\dot{\varepsilon} > 10^6$ (surface) in all simulations.

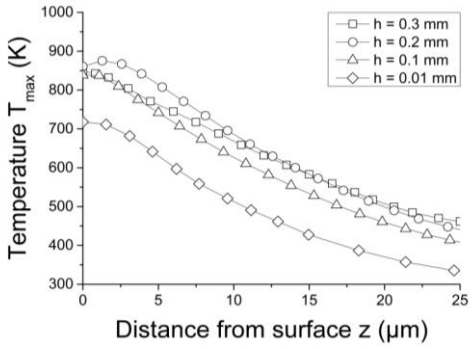

Fig 10. Maximum temperature at K = 1, and different cutting depths h after 1 mm length of cut.

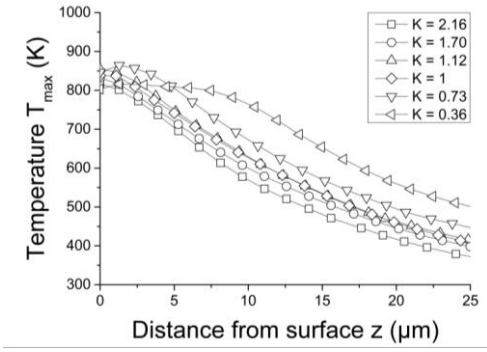

Fig 11. Maximum temperature for different K and cutting depth h = 0.1 mm after 1 mm length of cut.

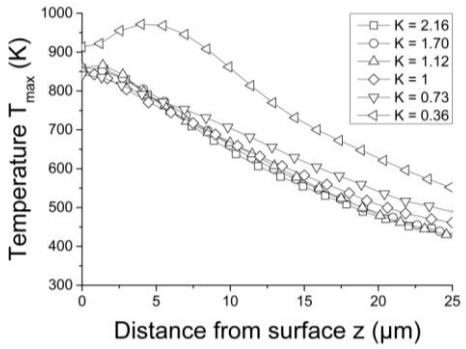

Fig 12. Maximum temperature for different K, and cutting depth h = 0.3 mm after 1 mm length of cut.

While the enhancing effect of low form-factor on temperatures can still be seen at 0.1 mm cutting depth (Fig 11), it results in a deeper affected layer depth rather than a higher peak temperature. In this case, the form-factor of 0.73 features the highest maximum temperature about 1.5 µm beneath the surface. The effect of asymmetry on the resulting temperature thus seems to be dependent not just on the microgeometry itself, but also on the cutting depth. This is due to a part of the shear bands moving below the cutting edge at low form-factors. The maximum temperatures below the surface reported in Fig 11 and 11 originate from this.

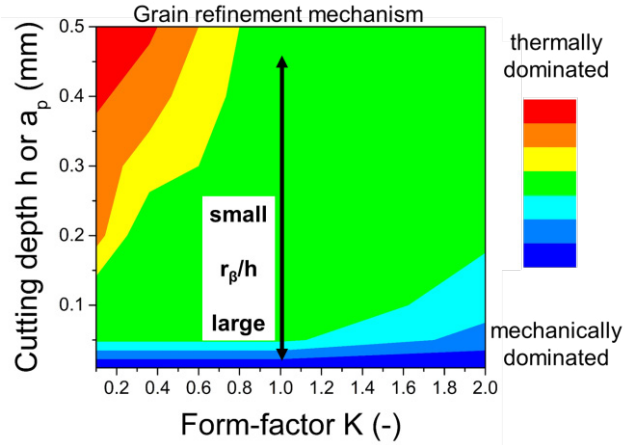

Fig 13. Sketch of a grain-refinement mechanism-map dependent on form-factor and cutting depth, extrapolated from simulations and experiments.

When considering the experimentally observed grain refinement at a form-factor of 0.36 in conjunction with the only other significant difference, namely the maximum temperatures within the surface layer during simulations, it seems that grain refinement in this case is driven thermally rather than mechanically. While this trend can also be seen at a form-factor of 0.73, results from the simulations suggest, that a critical thermal load for enhanced grain refinement would not be reached in this case. Higher relative roundness leads to a deeper affected surface layer mainly through mechanical effects while featuring the lowest overall temperature.

From the results of this work, a first draft of a mechanism-map for the thermo-mechanical process of grain refinement can be sketched as shown in Fig 13. It shows, that the grain refinement is almost independent of form-factor at small cutting depths and mechanically dominated. Increasing cutting depths then lead to more thermally dominated grain refinement at small form-factors, while increasing form-factor preserves the mechanical dominance.

5. Summary and outlook

Grain refinement of Ti6Al4V within the newly generated surface layer after machining has been subject of research both experimentally and in simulations. It is well known, that the driving mechanisms behind grain refinement are of both, mechanical and thermal nature. In this paper, the influence of asymmetric cutting edges, cutting depth, and relative roundness was investigated in experiments and simulations. Large relative roundness has been known to induce a ploughing effect, generating a deep layer of NC grains in steels. The same is found to be the case for Ti6Al4V in this work. Additionally, a form-factor of 0.36 leads to an even deeper layer affected by recrystallization. While the effect of relative roundness was found to be mostly mechanically driven, the effect of form-factor has a dominating thermal component. Additionally, this thermal effect is dependent on cutting depth, as it could be observed in simulations for a cutting depth of 0.3 mm but not at a cutting depth of 0.1 mm.

Future work will focus on enhancing the model in order to be able to quantitatively predict the NC and MC layer after machining. This will require careful consideration not just of the friction model, but also of the model to be used to calculate thermally and mechanically induced changes in grain size, which are available from literature. The result of this work suggests, that such a model needs to be able to be both, mechanically and thermally driven. While physics based models exist, it is not clear whether or not they can cope with both extremes shown in this work. Furthermore, the complex interaction of the dimensionless form-factor and cutting depth needs to be investigated with regard to the size of the microgeometries (e.g. ploughing zone height or other size-dependent features) and cutting speeds, both experimentally and in further simulations. This will enable the refinement of the mechanism-map sketched in this work.

In addition to considerations of grain refinement mechanisms, the observed influence of asymmetry is also of high importance when considering phase transitions. With regard to Ti6Al4V, the α to β transformation may start as about 870 K are reached for a sufficient duration. Obviously, this, may well be surpassed in the surface layer when using cutting edges with a very small form-factor at a sufficient cutting depth.

Acknowledgements

The authors would like to thank the German BMWi for funding the experimental and analytical work within the scope of the project FAWIBO (20Y1505C), headed by Liebherr Aerospace.

References

[1] Özel T, Ulutan, D. Prediction of machining induced residual stresses in turning of titanium and nickel based alloys with experiments and finite element simulations. CIRP Ann-Manuf Techn 2012;61:547-550.

[2] Umbrello D, Bordin A, Imbrogno S, Bruschi S. 3D finite element modelling of surface modification in dry and cryogenic machining of EBM Ti6Al4V alloy. CIRP-JMST 2016;18:92-100.
[3] Buchkremer S, Klocke F. Modeling nanostructural surface modifications in metal cutting by an approach of thermodynamic irreversibility. Continuum Mech Therm 2017;29:271-289.
[4] Denkena B, Koehler J, Rehe M. Influence of the Honed Cutting Edge on Tool Wear and Surface Integrity in Slot Milling of 42CrMo4 Steel. Procedia CIRP 2012;1:190–195.
[5] Maiss O, Grove T, Denkena B. Influence of asymmetric cutting edge roundings on surface topography. Production Engineering 2017;11(4-5):383-388.
[6] Segebade E; Zanger; Schulze V: Influence of Different Asymmetrical Cutting Edge Microgeometries on Surface Integrity. Procedia CIRP 2016;45:11-14.
[7] Wyen C-F, Knapp W, Wegener K. A new method for the characterisation of rounded cutting edges. Int J Adv Manuf Tech 2012;59:899-914.
[8] Ambrosy F, Zanger F, Schulze V. FEM-simulation of machining induced nanocrystalline surface layers in steel surfaces prepared for tribological applications. CIRP Ann-Manuf Techn 2015;64(1):69-72.
[9] Shivpuri R, Hua J. Microstructure-Mechanics Interactions in Modeling Chip Segmentation during Titanium Machining. CIRP Ann-Manuf Techn 2002;51(1):71-74.
[10] Johnson GR, Cook WH. Fracture Characteristics of three metals subjected to various strains, strain rates, temperatures and pressures. Eng Fract Mech 1985;21(1):31-48.
[11] Sun J; Guo Y: Material flow stress and failure in multiscale machining titanium alloy Ti-6Al-4V. Int J Adv Manuf Tech 2009;41:651-659.